Acoustical source-receiver intrefacing using the Patch Impedance Approach

L. Du et G. Pavic
LVA, INSA de Lyon, 25 bis av. Jean Capelle, 69621 Villeurbanne, France
liangfen.du@insa-lyon.fr

The analysis of sound field created by a sound source can be carried out by analysing separately the source and the receiving space and then by coupling the two using impedance rules. The source is then characterised by its blocked pressure while the coupling is done via an interface surface which fully encompasses the source. The sound field is finally obtained by fulfilling the continuity conditions across the interface surface. To enable numerical realisation of this approach the interface surface is discretised into patches and the field is then computed using classical matrix calculus. The paper addresses the following points of the modelling procedure : 1) Find the appropriate patch size ; 2) Assess the influence of random noise added to the source/receiver impedance and blocked pressure on the predicted responses ; 3) Find out the influence of system parameters on the predicted response ; 4) Predict the pressure response when the interface is a complex surface. A number of examples will be shown to illustrate the proposed approach.

1 Introduction

One of the most frequently used techniques for noise reduction of industrial products consists in analyzing noise radiation and trying out different ways to minimize the noise level. The disadvantage is long productive circle and high cost. In the past decades, Virtual acoustical prototype (VAP) [1], as a new noise reduction technique, has increasingly attracted researchers' attention because of its convenience and economy. The main idea of VAP is fulfilling noise reduction during the design stage of manufacture with the help of source models. Thus, finding an appropriate source model is a crucial step of VAP with the objective of predicting the sound field of a real source.

M. Ochmann [2] proposed the source simulation technique for acoustic radiation problems and proved the theoretical possibility of modeling the sound field of complex sources by simpler alternative sources. A. T. Moorhouse and G. Seiffert [3] used four monopoles to simulate the sound field around a motor in the semi-free field. However, one disadvantage of the equivalent source system is the dependence of the system on the acoustical environment. Y. I. Bobrovnitiskii and G. Pavic [4] introduced a concept of envelope surface to characterize the source via its *blocked pressure* and *source impedance*. Such an interface surrounding a source is always the same, no matter in which acoustical environment this source resides. The blocked pressure response is the pressure response on the rigid interface surface due to the source operating. The impedance of the interface with the idle source is the source impedance. The sound field in any acoustical environment is predicted with the help of the source's blocked pressure and source impedance. G. Pavic [5] then outlined how an available approach – Patch Impedance Approach - can be applied to measurements using planar interfaces.

The interface is sectioned into several patches which divides the acoustical environment into two independent spaces - source space with source and receiver space without source. In the source space, the pressure response from the operating source averaged across every patch in the blocked interface state gives blocked pressure vector. The pressure/velocity ratio of all patch combinations gives source impedance matrix. On the basis of Ref. [4] and [5], this paper assesses the scope and the limitation of patch impedance approach. An inadequate patch size may bring unacceptable differences between the predicted and real responses. The patch approach uses the values of sound field averaged across patch surface. Smaller patch size means larger number of patches and thus larger matrix dimension, leading to increased ill-conditioning. On the other hand, larger patches increase loss of information due to patch averaging. Hence an appropriate patch size is essential for the sound prediction.

This paper takes a simple model - sound radiation in a rectangular room - as a starting research step to find an optimum patch size using the Patch Impedance Approach. It then discusses the influence of measurement noise on the patch size. The third part deals with the influence of mesh size when using numerical computation. At the end, two sound prediction cases are analysed to check whether patch impedance approach gives acceptable predicted results. This analysis is carried out in frequency domain.

2 Conception

2.1 Blocked pressure and source/reciever impedance

The first step of patch impedance approach is creating an interface which divides the acoustic environment into two independent spaces : source space and receiver space, as shown in Fig. 1.

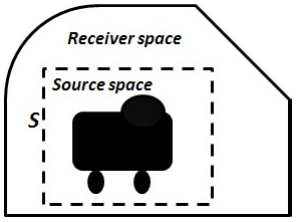

FIGURE 1 – Interface

The interface is divided into N patches. The blocked pressure is averaged across each patch of the interface, that is

$$P_b = (< p_{b1} >_{\triangle S}, \cdots, < p_{bi} >_{\triangle S}, \cdots < p_{bN} >_{\triangle S})^{\mathbf{T}} \qquad (1)$$

Here, N is number of patches, $\triangle S$ is patch area, $< \bullet >_{\triangle S}$ means $\frac{1}{\triangle S}\int_{\triangle S} \bullet dS$ and $< p_{bi} >_{\triangle S}$ is the pressure averaged across the i^{th} patch. The source impedance Z_s and the receiver impedance Z_r characterize acoustical properties of source and receiver spaces. With the source switched off and a volume velocity $< v_k >_{\triangle S}$ applied to the k^{th} patch, the pressure response $< p_{jk} >_{\triangle S}$ across the j^{th} patch is computed. This gives the $j-k$ element of the impedance matrix - $(Z_s)_{jk}$ or $(Z_r)_{jk}$, see Fig. 2 :

$$(Z_{s|r})_{jk} = \frac{< p_{jk} >_{\triangle S}}{< v_k >_{\triangle S}} \quad j,k = 1, \cdots, N \qquad (2)$$

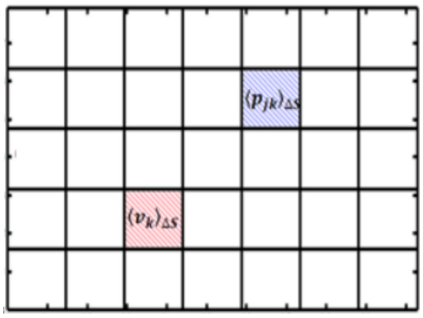

FIGURE 2 – Definition of source or receiver impedance

2.2 Coupling volume velocity

With blocked pressure and source/receiver impedance identified, the patch-averaged coupling volume velocity across the interface is :

$$V = (Z_s + Z_r)^{-1} P_b \tag{3}$$

The coupling velocity acts as an equivalent surface source radiating sound field in the receiver space. This enables predicting the sound pressure in any point of the receiver space.

3 Optimum patch size

3.1 The validity of Patch Impedance Approach

For the sake of simplicity of analytical computation the source is taken as 3 monopoles located at $(0.2, 0.22, 0.17)m$, $(0.48, 0.53, 0.59)m$, $(0.31, 0.65, 0.39)m$ in a rectangular room with $2.1 \times 1.0 \times 0.79m^3$, as shown in Fig. 3. The volume velocities of the monopoles are 1, -1, i m^3/s, respectively, with i – imaginary unit. We predict the sound field due to these monopoles in the room by patch impedance approach. The sound speed of air is $343m/s$, the air mass density is $1.21m/s$, the absorption coefficient of room is 0.01. A simple interface consisting of a single plane surface is set at $x = 0.79m$ seperating the room into source space and receiver space The interface is divided into several patches, as shown in Fig. 3.

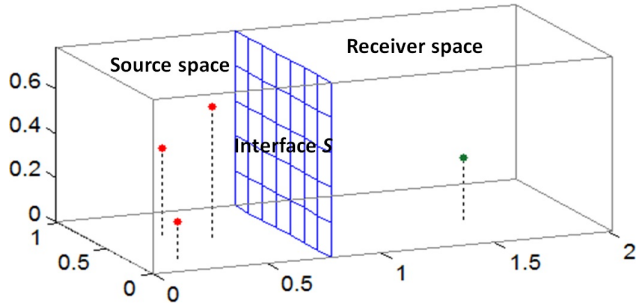

FIGURE 3 – Source - receiver model information

Using Eqs. (1) - (3), one can get the pressure response at any position in the receiver space by patch impedance approach ; for the sake of result checking the response at the same position will be obtained by a direct computation too [6]. In order to distinguish the results from the two approaches, we call the former and latter approach '*substructuring*' and '*direct*', respectively. The *direct* result is taken as a reference. As an example, we take the pressure response at one point $(1.54, 0.43, 0.28)m$. The interface is divided into 4 groups of patches : 1×1, 2×2, 4×3, 8×6 (corresponding patch size is $0.90m$, $0.45m$, $0.26m$, $0.13m$).

The two kinds of responses are shown in Fig. 4. The smaller the patch size, the better the substructured response matches the direct one in terms of the overall values. Moreover, the smaller the patch size, the higher the frequency above which the deviation of the substructuring method starts fluctuating substantially, as indicated by the vertical dotted dash lines in Fig. 4. In other words, the patch size should be smaller to get better matching at higher frequencies.

3.2 Characterisation error

We will find the relation between the appropriate patch size (d_{appr}) and minimum wavelength (λ_{min}) on the basis of a case study. Take the model in Fig. 3 and let the patch size (d) decrease from 0.90m ($> \lambda_{min}$) to 0.09m ($\leq \frac{1}{7}\lambda_{min}$). More detailed information is given in Tab. 1. The frequency band is [1, 500]Hz and the minimum wavelength (λ_{min}) is $0.68m$. According to Ref. [5], the patch averaged substructured pressure response at the interface P in the receiver space can be computed by :

$$P = Z_r(Z_s + Z_r)^{-1} P_b \tag{4}$$

Substituting Eq. (1) and Eq. (2) into Eq. (4) yields $P = (< p_1 >_{\Delta S}, \cdots, < p_i >_{\Delta S}, \cdots < p_N >_{\Delta S})^{\mathbf{T}}$. Here, $< p_i >_{\Delta S}$ is the coupling pressure response averaged across the i^{th} patch.

The vibrating interface acts as an equivalent source in the reveiver space, which reproduces sound field radiated by the original source. If the patch size is appropriate, the substructured volume velocity averaged across each patch over the interface almost equals to the exact volume velocity across the same patch. The predicted sound field must then get close to the exact one. The following equation will be used to assess the influence of the patch size on the predicted response.

$$\epsilon(d, f) = \sqrt{\frac{\frac{1}{N}\sum_{i=1}^{i=N} |\langle p_i(\mathbf{r}_i, f)\rangle_{\Delta S} - \langle \widetilde{p_i}(\mathbf{r}_i, f)\rangle_{\Delta S}|^2}{\frac{1}{N}\sum_{i=1}^{i=N} |\langle \widetilde{p_i}(\mathbf{r}_i, f)\rangle_{\Delta S}|^2}} \tag{5}$$

Here, ϵ is *characterisation error*, f is frequency, $\mathbf{r}_i$ is the center position of the i^{th} patch, $\langle p_i(\mathbf{r}_i, f)\rangle_{\Delta S}$ is the substructured pressure response averaged across the i^{th} patch, $\langle \widetilde{p_i}(\mathbf{r}_i, f)\rangle_{\Delta S}$ is the exact pressure response averaged across the same patch.

Fig. 5 shows the characterisation error ϵ of cases in Tab. 1 according to patch size d and frequency f. Fig. 5(a) demonstrates that at low frequencies, the characterization error almost stays the same as the patch size decreases, except to a very small extent at resonance and anti-resonance frequencies. So the largest patch of the 15 cases is still small enough to get a globally good substructured result. On the contrary, at middle and high frequencies, the characterization error varies a lot with the patch size, especially when the patch size is larger than $\frac{1}{3}\lambda_{min}$, as shown by the second plot in Fig. 5(a). Fig. 5(b) shows the characterisation error changing as the patch size at some fixed frequencies. At a fixed frequency the decrease in patch size below some given value will not further reduce the characterisation error.

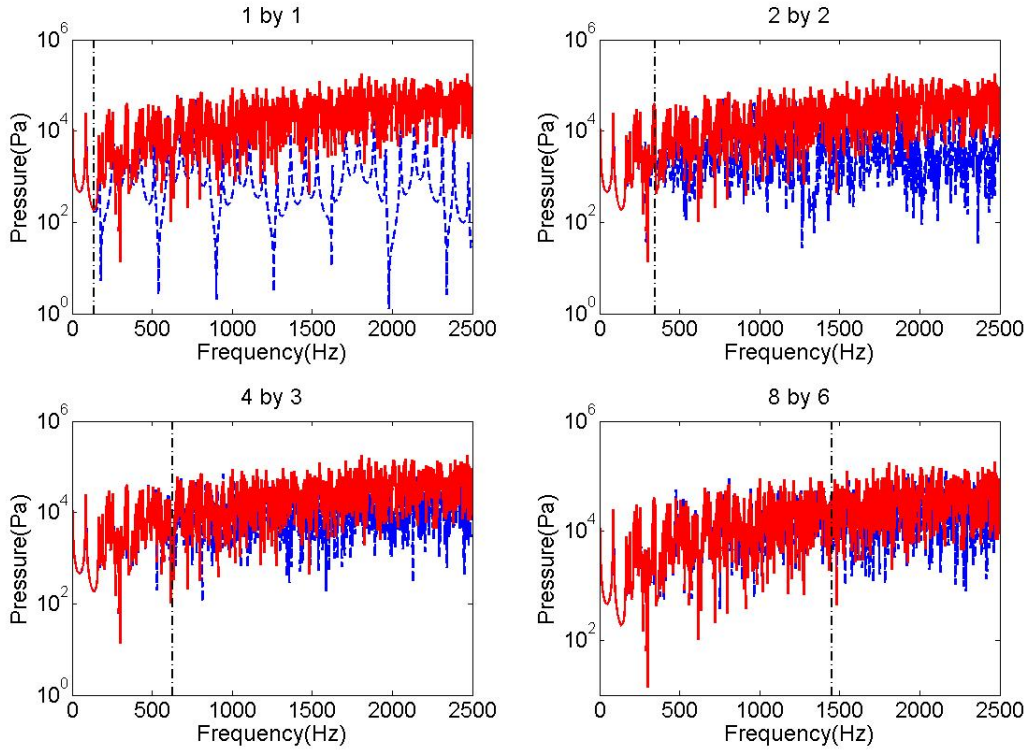

FIGURE 4 – Pressure responses at $(1.54, 0.43, 0.28)m$ while the patch size is $0.90m$, $0.45m$, $0.26m$, $0.13m$, respectively. The solid line is the direct response while the dashed line is the substructured response. The vertical line indicates the start of unacceptable error.

The patch size corresponding to that value is the optimum patch size. The optimum can be explained by two effects : (1) when the patch size is larger than the optimum size, the predcted result varies a lot with the size, which means that the result is not reliable ; (2) when the patch size is smaller than the optimum patch size, the characterisation error is not reduced. Because smaller patch size means larger computation or more measuring work in reality, the optimum patch size makes the work more efficient. After checking and analysing the optimum patch sizes at all frequencies, it appears that the size of $\frac{1}{3}\lambda$ is a turning point where the characterisation error starts to converge. For example, the optimum patch sizes at 6 frequencies in Fig. 5(b) are $0.90m$, $0.45m$, $0.45m$, $0.3m$, $0.26m$, $0.2m$, the ratios of the optimum patch size and wavelength are 0.43, 0.43, 0.28, 0.36, 0.42, 0.33, 0.27. In short, $\frac{1}{3}\lambda$ can be considered as a good compromise criterion for choosing the optimum patch size.

3.3 Influence of noise on characterisation error

In real applications, the blocked pressure and source/receiver impedance would be obtained by measurements. Measurement noise is an uncertain factor during the sound prediction which may yield large error in the predicted results. Is the accuracy of sound prediction results based on patch impedance approach more sensitive to the patch size while measurement noise exists ? Is $\frac{1}{3}\lambda$ still the appropriate patch size in these conditions ? In this section, we will discuss the influence of random noise on the patch size.

TABLEAU 1 – 15 different cases

Case	Number of patches, N	Patch size,$d(m)$	$\frac{d}{\lambda_{min}}$
1	11×9	0.09	$\leq \frac{1}{7}$
2	10×8	0.10	$\left(\frac{1}{7}, \frac{1}{6}\right]$
3	9×7	0.11	
4	8×6	0.13	$\left(\frac{1}{6}, \frac{1}{5}\right]$
5	7×6	0.14	$\left(\frac{1}{5}, \frac{1}{4}\right]$
6	7×5	0.15	
7	6×5	0.16	
8	6×4	0.18	$\left(\frac{1}{4}, \frac{1}{3}\right]$
9	5×4	0.20	
10	4×3	0.26	$\left(\frac{1}{3}, \frac{1}{2}\right]$
11	3×3	0.30	
12	3×2	0.37	$\left(\frac{1}{2}, 1\right]$
13	2×2	0.45	
14	2×1	0.64	
15	1×1	0.90	> 1

According to the definition of impedance $Z = \frac{P}{V}$, volume velocity V is an input signal, pressure P is an output signal and impedance is a transfer function. In the presence of noise the transfer function Z at a given frequency will read

$$Z = \frac{P + W_p}{V + W_v} \tag{6}$$

Where W_p and W_v are the amplitudes of noise signals added to pressure and velocity signals respectively. The simulation will be done by selecting an overall signal-to-noise value for pressure and velocity signals and then distributing the noise amplitudes uniformly over the frequency span while giving

$$\hat{\epsilon}(d,f,SNR1,SNR2) = \sqrt{\frac{\frac{1}{N}\sum_{i=1}^{i=N}|\langle\hat{p}_i(\mathbf{r}_i,f,SNR1,SNR2)\rangle_{\triangle S} - \langle\widetilde{p}_i(\mathbf{r}_i,f,SNR1,SNR2)\rangle_{\triangle S}|^2}{\frac{1}{N}\sum_{i=1}^{i=N}|\langle\widetilde{p}_i(\mathbf{r}_i,f,SNR1,SNR2)\rangle_{\triangle S}|^2}} \quad (7)$$

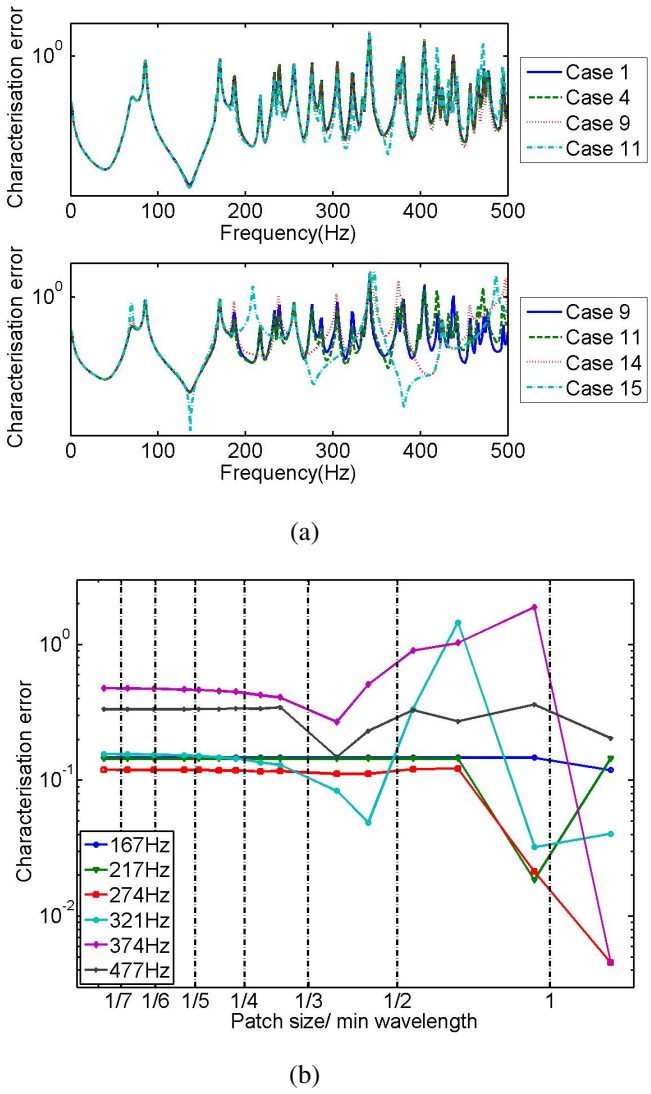

FIGURE 5 – Characterisation error

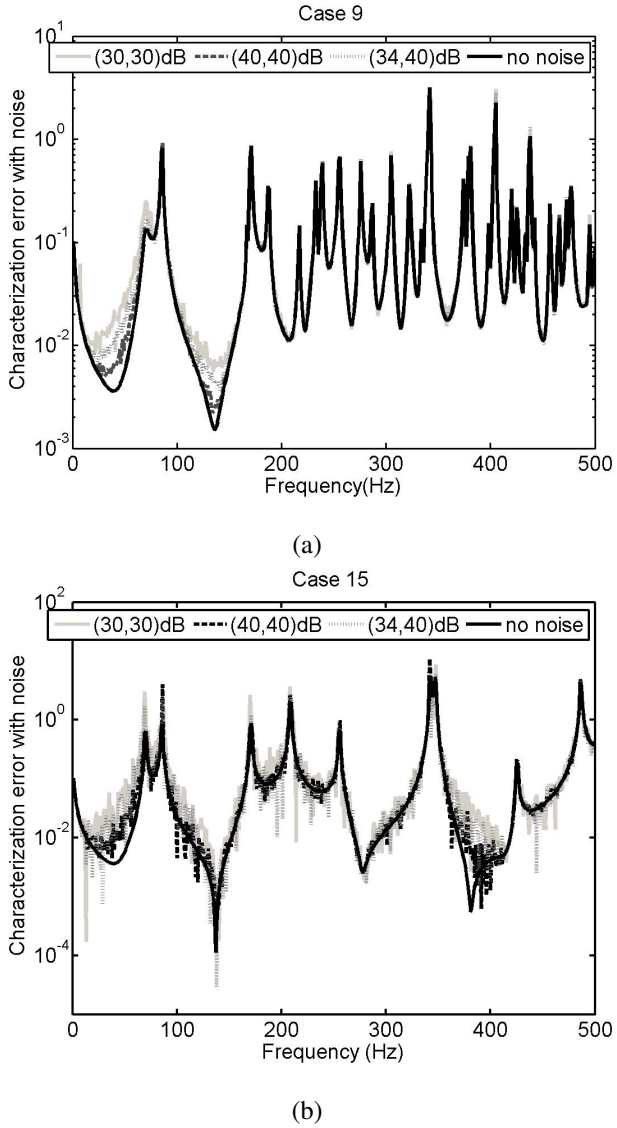

FIGURE 6 – $\hat{\epsilon}(f,SNR1,SNR2)$

random values to the phases. Denoting the decibel values of the signal-to-noise ratios of pressure and velocity signals by $SNR1$ and $SNR2$, the substructured pressure response $\langle p_i(\mathbf{r}_i,f)\rangle_{\triangle S}$ in Eq. (5) becomes $\langle\hat{p}_i(\mathbf{r}_i,f,SNR1,SNR2)\rangle_{\triangle S}$. Upon inserting it into Eq. (5), the characterisation error with noise $\hat{\epsilon}(d,f,SNR1,SNR2)$ is obtained, see Eq. (7). The characterisation error with noise of 10 cases in Tab.1 will be analysed using $30dB$, $32dB$, $34dB$, $36dB$, $38dB$, $40dB$ of $SNR1$ and $SNR2$.

Take Cases 9 and 15 as examples. When patch size d is fixed and $(SNR1,SNR2)$ is $(30,30)$, $(34,40)$, $(40,40)dB$, $\hat{\epsilon}$ is shown in Fig.6. For Case 9, $\hat{\epsilon}$ is close to ϵ, except a little larger at low frequencies ; for Case 15, $\hat{\epsilon}$ fluctuates around ϵ.

Fig. 7 shows the error of a fixed f. (SNR1, SNR2) changes from $(30,30)dB$ to $(40,40)dB$ by $2dB$ step. d changes from $0.15m$ to $0.9m$, $\hat{\epsilon}$ is almost equal to ϵ.

In summary, Fig. 6 and Fig. 7 demonstrate that the noise has relatively secondary influence on characterisation error, which means $\frac{1}{3}\lambda$ can still be considered as the optimum patch size.

4 Influence of system parameters

A rectangular box surface is the most suitable interface for the sound prediction with respect to the pratical experiment. Such a surface connot be handled analytically. A numerical method, such as FEM, has to be used for better clarifying limitations, i.e. the distance between the source and the interface. Before going into the analysis, we have to make sure the mesh size of numerical model is small enough. Normally, $\frac{1}{6}\lambda_{min}$ is the criterion of choosing mesh size, but it is unknown whether this criterion fits our computation using patch impedance approach.

In the example shown in Fig. 8, a rectangular room is $2m \times 1.2m \times 2m$, a point source is at $(0.2, 0.38, 0.55)m$ and its pressure amplitude is 1 Pa. The interface is at $x = 0.7m$. The frequency band is [200, 300]Hz. The appropriate patch size, as discussed in the previous section, sets the patch to $0.2m \times 0.2m$ so the interface is divided into 30 patches. The substructured pressure response averaged across all

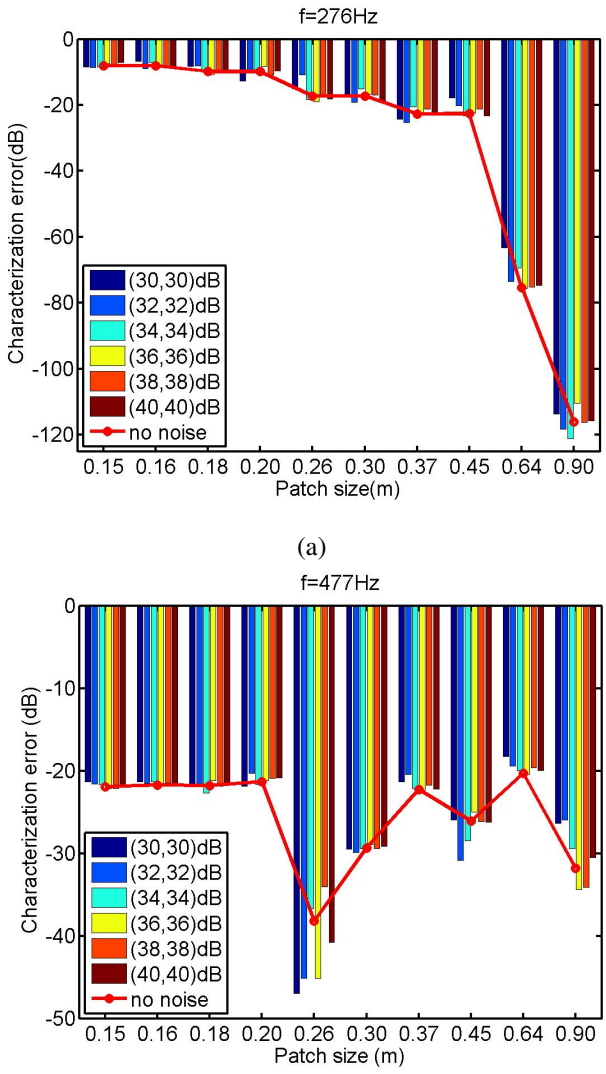

FIGURE 7 – $\hat{\epsilon}(d, SNR1, SNR2)$

patches in the receiver space is computed by two methods - numerical method and analytical method - both using patch impedance approach. The response obtained by analytical method is the reference result. This numerical model is created by Hypermesh and Frequency Response Analysis is done by Actran.

Using the mesh sizes of $\frac{1}{6}\lambda_{min}$, $\frac{1}{9}\lambda_{min}$, $\frac{1}{12}\lambda_{min}$, $\frac{1}{15}\lambda_{min}$, $\frac{1}{18}\lambda_{min}$, 5 pressure responses averaged across the patch centred at $(0.7, 0.9, 1.1)m$ at [256, 263]Hz by 0.05Hz step are shown in Fig. 9. As this figure illustrates, the response is closer to the reference one with the mesh size declining. It seems that the numerical method causes a frequency shift which descends gradually as the mesh size decreases. The frequency shifts at resonance frequencies in [256, 263]Hz compared with the reference resonance frequency are listed in Tab. 2. The pressure amplitudes at resonance frequencies change little with the mesh size, but the frequency shift when mesh size is $\frac{1}{6}\lambda_{min}$ is about 4 times as that when mesh size is $\frac{1}{18}\lambda_{min}$. So the smaller the mesh size, the smaller the frequency shift. The inconvenience of frequency shift can be removed if the frequency response analysis is done in frequency bands. In such a case, the $\frac{1}{6}\lambda_{min}$ criterion remains adequate.

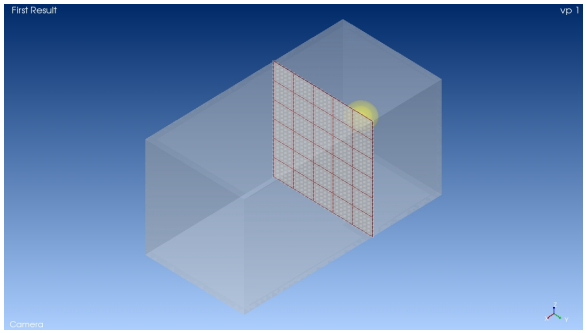

FIGURE 8 – Basic model

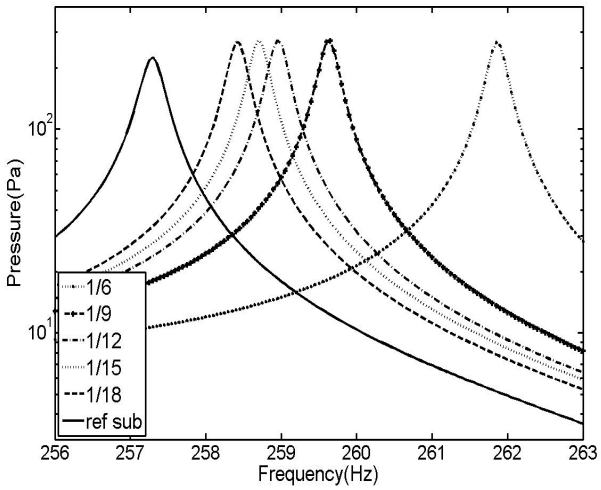

FIGURE 9 – Pressure response at the patch centered at $(0.7, 0.9, 1.1)m$

5 Complex interface

We use two more complex interfaces - a box and a semi-cylinder - to predict the sound field in a room in Fig. 10. All the properites of the room are the same to those used in Section 4, except the source position and the interface. The mesh size is $\frac{1}{18}\lambda_{min}$ and the patch size is about $\frac{1}{3}\lambda_{min}$. The interface box is $1m$ length, $0.5m$ width, $0.6m$ height and its center is at $(1, 0.5, 1)m$, while the radius and height of the semi-cylinder is $0.3m$ and $1.2m$ and its central axis is at $x = 0.775m$. The source positions in the box and the semi-cylinder are at $(1, 0.5, 0.6)m$ and $(0.775, 0.15, 0.6)m$. The responses at $(0.3, 0.2, 0.15)m$ in the box case and at $(1.816, 0.6058, 0.7072)m$ in the cylinder case are shown in Fig. 11. The predicted result is found to match well the exact

TABLEAU 2 – Amplitude error and frequency shift at a resonance frequency in [256, 263]Hz

mesh size/λ_{min}	pressure amplitude (Pa)	amplitude error (dB)	resonance frequency (Hz)	frequency shift(%)
ref	224.92	–	257.3	–
$\frac{1}{6}$	265.73	3.33	261.85	1.77
$\frac{1}{9}$	271.80	3.79	259.65	0.91
$\frac{1}{12}$	272.90	3.87	258.95	0.64
$\frac{1}{15}$	273.72	3.93	258.7	0.54
$\frac{1}{18}$	267.14	3.44	258.4	0.43

one even though the interfaces are complex.

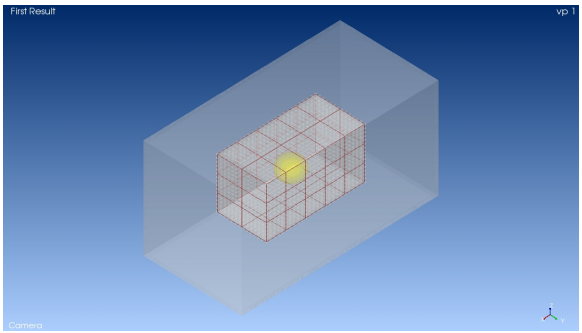

(a) Box

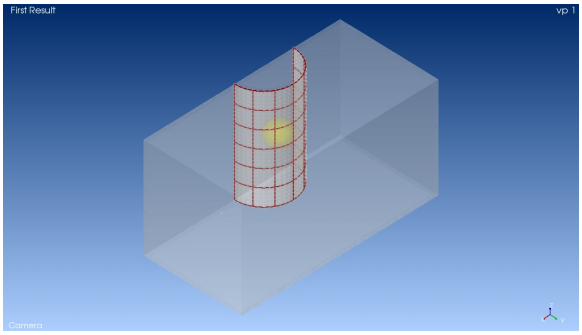

(b) Semi-cylinder

FIGURE 10 – Complex interface

6 Conclusions

From the above discussion, we conclude that (1) $\frac{1}{3}\lambda$ is the optimum patch size ; (2) the smaller the mesh size is, the smaller the frequency shift is. If the frequency response analysis is fulfilled in frequency bands, the $\frac{1}{6}\lambda_{min}$ criterion is adequate regarding the patch approach ; (3) patch approach can give acceptable results even though the interface is complex. In future, more complex cases of source geometry and positioning will be studied for better understanding the limitations of the substructuring technique using Patch Impedance Approach.

Acknowledgements

The authors would like to thank China Scholarship Council for financial support.

Références

[1] A. Moorhouse, Virtual acoustic prototypes : listening to machines that don't exist, *Proceeding of Acoustics*, 9-11, Western Australia(2005).

[2] M. Ochmann, The source simulation technique for acoustic radiation problems, *Acustica*, **81**, 512-527 (1995).

[3] A. T. Moorhouse and G. Seiffert, Characterisation of an airborne sound source for use in a virtual acoustic prototype, *Journal of Sound and Vibration* , **296**, 334-352 (2006).

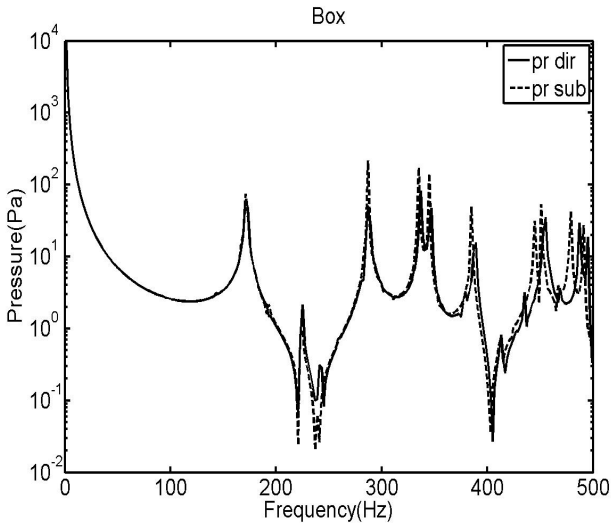

(a) Box

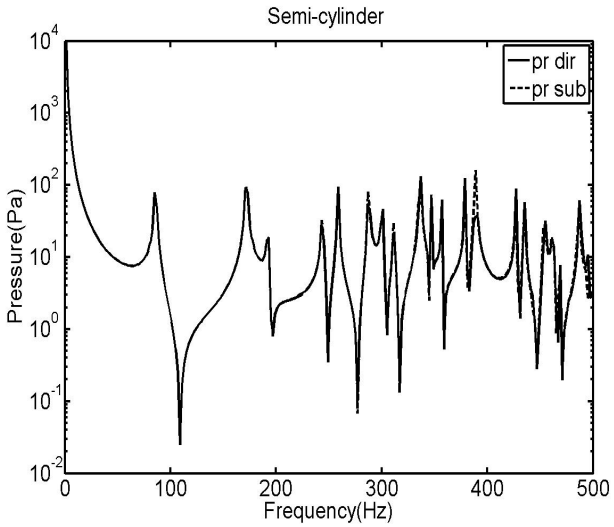

(b) Semi-cylinder

FIGURE 11 – Pressure responses at two points in two receiver spaces

[4] Y. I. Bobrovnitskii and G. Pavic, Modeling and characterization of airborne noise sources, *Journal of Sound and Vibration* , **261**, 527-555 (2003).

[5] G. Pavic, Air-borne sound characterization by patch impedance coupling approach, *Journal of Sound and Vibration* , **329**, 4907-4921 (2010).

[6] H. Kuttruff, *Room acoustic(Fifth edition)*, Spon Press (2009).